HHS Public Access

Author manuscript

J Immunol. Author manuscript; available in PMC 2016 August 04.

Published in final edited form as:

J Immunol. 2016 June 1; 196(11): 4622–4631. doi:10.4049/jimmunol.1502452.

Dual function of Ccr5 during Langat virus encephalitis - Reduction of neutrophil-mediated CNS inflammation and increase in T cell-mediated viral clearance

Daniela Michlmayr[*,1], **Susana V. Bardina**[*,1], **Carlos A. Rodriguez**[*], **Alexander G. Pletnev**[†], and **Jean K. Lim**[*,‡]

[*]Department of Microbiology, Icahn School of Medicine at Mount Sinai, One Gustave L. Levy Place, Box 1124, New York, NY 10029

[†]Laboratory of Infectious Diseases, National Institute of Allergy and Infectious Diseases, National Institutes of Health, Bethesda, MD 20892

Abstract

Tick-borne encephalitis virus (TBEV) is a vector-transmitted flavivirus that causes potentially fatal neurological infection. There are thousands of cases reported annually, and despite the availability of an effective vaccine, the incidence of TBEV is increasing worldwide. Importantly, up to thirty percent of affected individuals will develop long-term neurologic sequelae. We investigated the role of chemokine receptor Ccr5 in a mouse model of TBEV infection using the naturally attenuated tick-borne flavivirus, Langat virus (LGTV). Ccr5-deficient mice presented with an increase in viral replication within the CNS and decreased survival during LGTV encephalitis when compared to wild type (WT) controls. This enhanced susceptibility was due to the temporal lag in lymphocyte migration into the CNS. Adoptive transfer of WT T cells, but not Ccr5-deficient T cells, was able to significantly improve survival outcome in LGTV-infected Ccr5-deficient mice. Concomitantly, a significant increase in neutrophil migration into the CNS in LGTV-infected *Ccr5*$^{-/-}$ mice was documented at the late stage of infection. Antibody-mediated depletion of neutrophils in *Ccr5*$^{-/-}$ mice resulted in a significant improvement in mortality, a decrease in viral load, and a decrease in overall tissue damage in the CNS when compared to isotype control-treated mice. Ccr5 is crucial in not only directing T cells towards the LGTV-infected brain, but also in suppressing neutrophil-mediated inflammation within the CNS.

INTRODUCTION

Tick-borne encephalitis virus (TBEV), a neurotropic flavivirus, is predominantly transmitted through the bite of an infected tick and can cause tick-borne encephalitis (TBE) (1–3). The

[‡]Corresponding author: Jean K. Lim, Department of Microbiology, Icahn School of Medicine at Mount Sinai, One Gustave L. Levy Place, Box 1124, New York, NY 10029; jean.lim@mssm.edu; telephone: +1-212-241-7811; fax: +1-212-534-1684.

[1]Daniela Michlmayr and Susana V. Bardina contributed equally to this work and are co-first authors

AUTHORSHIP Contributions: D.M., S.V.B, and J.K.L. conceived and designed the experiments and wrote the manuscript; D.M., S.V.B, C.A.R., and J.K.L. conducted the experiments, assembled and analyzed the data, and interpreted the results; A.G.P. provided technical assistance and provided key reagents; all authors reviewed and comments on the manuscript and approved the final version.

CONFLICT OF INTEREST DISCLOSURE The authors declare no competing financial interests.

outcome of TBEV infection is dependent on various factors, including the type and strain of TBEV, age, immune status, and genetic predisposition. Upon infection, approximately 70% of individuals will remain asymptomatic, with the remaining individuals developing a febrile illness that can potentially progress to meningitis and/or encephalitis and death (2–4). Thirty percent of patients who develop TBE suffer from long-term neurological sequelae and often require prolonged rehabilitation. The fatality rate ranges between 2%, caused by the European subtype, and 40% for the Far Eastern subtype (1, 5). Despite the availability of a vaccine, there are approximately 15,000 cases of TBE reported annually, with ~3,000 cases in Europe and the remainder reported in Russia (1, 2, 6, 7). Currently, there are no specific antiviral treatments for TBEV, and a better understanding of pathogenesis is required for the development of targeted therapies.

A hallmark of viral encephalitis is the accumulation of leukocytes in the infected CNS, which is essential for viral clearance but can also lead to neuroimmunopathology (8) (9). Leukocyte migration into infected tissues is guided, in part, by chemokines produced during inflammation, with their receptors found on circulating leukocytes. In the context of numerous inflammatory conditions, the chemokines Ccl3, Ccl4, and Ccl5 are induced both early and to high levels in the periphery and within the CNS. The common receptor for these ligands, chemokine receptor Ccr5, is expressed by a wide range of leukocytes, including activated T cells, natural killer (NK) cells, and monocytes/macrophages, and it has been shown to have a critical role in neuroprotection against *Cryptococcus neoformans*, HSV-2, and most recently, neurotropic flaviviruses (10–16). In a murine model of West Nile virus (WNV) infection, Ccr5 was shown to be a critical antiviral and survival determinant; in Ccr5-deficient mice, viral replication was uncontrolled within the CNS, which was concomitant with the global loss of infiltrating peripheral leukocytes into the infected CNS (17). The protective role of Ccr5 in mice has been translated in cohorts of WNV-infected individuals where *CCR5Δ32* homozygosity, rendering individuals CCR5-deficient, was associated with increased risk of developing symptomatic WNV disease; conversely, CCR5 deficient individuals were absent from asymptomatic WNV-infected blood donors (11, 18, 19). In a related mouse model of Japanese encephalitis virus (JEV) infection, *Larena et.al* found that Ccr5-deficient mice exhibited increased viral titers in the CNS and enhanced mortality compared to wild type (WT) mice that was due to impaired trafficking and reduced functional activity of NK-cells and $CD8^+$ T cells in the CNS (13). Due to the relative absence of the *CCR5Δ32* allele in the human population in Asian countries where the majority of JEV cases occur, the ability to test the role of CCR5 in human genetic susceptibility to JEV is limited (20). Both WNV and JEV are mosquito-transmitted neurotropic flaviviruses that are related genetically and serologically. Currently, it is unclear whether the protective function of Ccr5 extends to more distantly-related, serologically-distinct neurotropic flaviviruses, such as the tick-borne flaviviruses.

In this study, we sought to understand the role of Ccr5 during TBEV infection. To address this, we used Langat virus (LGTV), which shares 78%–88% amino acid identity among the structural enveloped proteins of the tick-borne flaviviruses and was once considered as a live attenuated vaccine strain (2, 21–26). We found that efficient effector lymphocyte migration into the CNS was dependent on Ccr5; in the absence of this receptor, uncontrolled viral replication resulted in a dysregulation of neutrophil migration into the CNS, leading to

enhanced apoptosis. Our findings suggest that Ccr5 is a critical host response gene that contributes to maintaining a balance between the antiviral response and immunopathology within the CNS.

MATERIALS AND METHODS

Virus and virus quantification

Wild-type (WT) Langat virus strain TP21 (GenBank accession no. AF253419; http://www.ncbi.nlm.nih.gov/nuccore/AF253419) stock was generated in Vero cells (World Health Organization, passage 143) from a plaque-purified LGTV TP21 virus preparation, as described previously (24). To measure infectious virus, Vero cell monolayers in 24 well plates were infected with 100 μl of supernatants for 1 hour at 37°C. Cells were overlayed with 1 ml Opti-MEM (Invitrogen) containing 0.8% methylcellulose (Fisher scientific), 2% FBS, and 50 μg/ml Gentamicin sulfate. After a 3 day incubation, plates were fixed with 100% methanol. Antigen was detected with TBEV-specific antibodies (1:2500; ATCC), followed by staining with goat anti-mouse IgG antibodies (1:500; Invitrogen) conjugated with horseradish peroxidase. LGTV focus forming units (FFU) were visualized by the addition of 1 ml 3,3'diaminobenzidine (DAB) tetrahydrochloride hydrate HRP substrate (Sigma). Viral RNA was isolated from mouse plasma using a QIAamp Viral RNA Mini Kit (Qiagen) and converted into cDNA using a Quantitect Reverse Transcription Kit (Qiagen) according to the manufacturer's protocol. For quantitative real-time PCR (qRT-PCR), the following primers were used: forward 5'-CAGTGGACACAGAGCGAATG-3'; reverse 5'-ACAGTCAGGTTTGCCTCACC-3'. The samples were run for 40 cycles using the Roche LightCycler 480 Real Time PCR System. The absolute copy number was calculated using a standard curve generated using a LGTV NS5-containing plasmid DNA.

LGTV infection model

Mouse studies were carried out in an animal biosafety level two facility under a protocol approved by the Icahn School of Medicine at Mount Sinai Animal Care and Use Committee. *Ccr5*$^{-/-}$ and WT C57BL/6J mice were purchased from the Jackson Laboratory. All experiments were initiated using female mice at 4 weeks of age. Mice were infected subcutaneously in the scruff of the neck with 10^6 FFU of LGTV suspended in 50 μl phosphate-buffered saline (PBS). Mice were monitored for morbidity and mortality for up to 18 days.

Immune cell analysis

Mice were deeply anesthetized with ketamine/xylazine prior to cardiac perfusion with ice cold PBS. Brains were removed aseptically, collected in 7 ml FACS buffer (PBS + 2% FBS), and homogenized using a dounce homogenizer. After the addition of 3 ml of 100% isotonic Percoll (GE Healthcare), the homogenate was underlayed with 1 ml of 70% isotonic Percoll. After centrifugation at 2470 rpm for 30 min at 4°C, cells at the interphase were washed in FACS buffer prior to antibody staining. Anti-coagulated blood was incubated with PharmLyse buffer (BD Biosciences) for 2 minutes on ice according to the manufacturer's protocol. UV live/dead cell stain kit (Invitrogen) was used to assess cell viability, and cells were blocked for non-specific Fc-mediated interactions with 0.5 ug purified anti-mouse

CD16/CD32 (BD Biosciences) for 20 minutes at 4°C prior to antibody staining. The following antibodies were used: CD3-FITC (17A2), CD8-PE (53.6.7), CD4-PerCp5.5 (GK1.5), Ly6C-FITC (HK1.4), Ly6G-PE (1A8), CD11b-APC (M1/70), CD45-APC-Cy7 (30-F11), NK1.1-PE (PK136) and CD19-APC (eBio1D3) (all from eBioscience). Data were collected using the LSR II flow cytometer (Becton-Dickinson) and analyzed using FlowJo software 8.5.3 (Treestar). Cell numbers were quantified using counting beads (Spherotech).

Protein quantification

Cytokines and chemokines were measured using a multiplex ELISA-based assay as previously described (27, 28). Briefly, antibodies and cytokine standards were purchased from R&D Systems or PeproTech. Individual Luminex bead regions were coupled to capture antibodies for each cytokine or chemokine measured. Biotinylated detection antibodies were used at twice the recommended concentration. Approximately 1200 beads were used for each cytokine or chemokine per sample. The plates were read on a Luminex MAGPIX system with at least 50 beads collected for each region per sample. The median fluorescence intensity was determined for analysis with the Milliplex software using a five-parameter regression algorithm.

Immunohistochemistry and TUNEL staining

Perfused brains were immediately fixed in 10% neutral buffered formalin (VWR) prior to paraffin embedding. 5–6 μm sections were rehydrated prior to antigen retrieval with citrate buffer as previously described (29). Slides were incubated with the primary antibody rat anti-mouse B220 (1:500, Biolegend) and mouse anti-TBEV (1:1000, ATCC) at 4°C overnight. The sections were then incubated with 2.5 μg/ml biotinylated anti-rat or anti-mouse IgG antibodies (Vector Laboratories) for 30 minutes at RT and incubated with the VECTASTAIN Elite ABC-peroxidase reagent (Vector Laboratories). Staining for CD3 (1:100, Vector Laboratories) and myeloperoxidase (1:1000, DAKO) was used in conjunction with the rabbit EnVision/HRP Kit (DAKO) according to the manufacturer's guidelines. All sections were visualized by incubating slides with DAB HRP substrate for 1–2 minutes at RT and counterstained with Gill's hematoxylin (Vector Laboratories) for 2 minutes. Sections were then dehydrated in a series of increasing ethanol concentrations and mounted with DPX mountant (Sigma). A terminal deoxynucleotidyl transferase dUTP nick-end labeling (TUNEL) assay was used to visualize apoptotic cells. For this, sections were stained using the DeadEnd Colorimetric TUNEL Systems Kit (Promega), then counterstained with Gill's hematoxylin for 2 minutes and mounted with 100% Glycerol (Sigma). The positive control slide was treated with DNase for 10 minutes at RT to introduce nicks in the DNA. All slides were analyzed using an AxioImager Z2 microscope (Zeiss) and the Zen 2012 software (Zeiss).

Adoptive Transfer studies

On day 8 post LGTV infection, T cells from spleens of *Ccr5*$^{-/-}$ and WT donor mice were enriched using the Pan T cell Isolation Kit II (Miltenyi) and the AutoMACS Magnetic Cell Sorter (Miltenyi) according to the manufacturer's guidelines. Enrichment resulted in ~85% CD45^{+}CD3^{+} T cell purity. On day 5 post infection, *Ccr5*$^{-/-}$ recipient mice were injected

intravenously (IV) with 10^6 T cells from either WT or *Ccr5*$^{-/-}$ donor mice in 100 μl PBS and monitored for survival for 18 days.

In vivo depletion of neutrophils

Neutrophils were depleted using anti-Ly6G antibody clone 1A8 (BioXCell); rat IgG2a isotype was used as a control. Briefly, 250 μg of anti-Ly6G or isotype control antibody in 100 μl PBS was injected intraperitoneally into each mouse on days 8, 10, and 12 post infection.

Statistical analysis

All data were analyzed using the Prism Version 5 software (GraphPad) and a Pearson Omnibus K2 and Shapiro-Wilks test was performed to test if data were normally distributed. In brief, a Student's unpaired *t* test or Mann-Whitney U test was performed. For all survival analyses, a Kaplan-Meier survival curve was generated, and statistical significance was determined using a log-rank test.

RESULTS

Ccr5 deficiency increases susceptibility to LGTV infection

To understand the role of Ccr5 in host defense during LGTV infection, we infected WT and *Ccr5*$^{-/-}$ mice subcutaneously with 10^6 FFU of LGTV strain TP21. While both WT and *Ccr5*$^{-/-}$ mice exhibited weight loss, lethargy, hunchback posture, and fur ruffling starting on day 7 post infection, only *Ccr5*$^{-/-}$ mice displayed signs of neurological disease, including unilateral or bilateral limb paralysis, severe disorientation, ataxia, and seizures. Consistent with these observations, *Ccr5*$^{-/-}$ mice exhibited a decreased survival (Figure 1A) compared to WT mice (48% in *Ccr5*$^{-/-}$ mice versus 90% in WT mice; p=0.0008). Daily evaluation of LGTV-infected *Ccr5*$^{-/-}$ mice showed a transient and significant increased weight loss on days 8 and 9 post infection compared to WT mice (Figure 1B).

Given the increased morbidity and mortality in the *Ccr5*$^{-/-}$ mice, we next examined viral burden in the periphery and CNS. Viremia on days 1, 3, 5, and 7 were similar between WT and *Ccr5*$^{-/-}$ mice (Figure 1C). Similarly, no differences in viral clearance were observed within the spleen (Figure 1D), demonstrating that viral clearance in the periphery was nearly identical between the two strains. In the CNS, initial viral loads were similar between WT and *Ccr5*$^{-/-}$ mice in both the brain and spinal cord. However, viral burden remained high in *Ccr5*$^{-/-}$ mice compared to WT mice in the brain on day 12 post infection (p=0.045) and spinal cord on day 10 post infection (p=0.034) (Figure 1E and F), which is consistent with the observed symptom onset. These data point to a protective, antiviral role for Ccr5 within the CNS.

Ccr5 does not alter the cellular or inflammatory response in the periphery during LGTV infection

Since depressed effector cell function can hinder viral clearance within the CNS, we investigated whether Ccr5 may be involved in the initiation of the cellular response to LGTV. To investigate this, we examined the role of Ccr5 on lymphocyte numbers in the

periphery of WT and *Ccr5*$^{-/-}$ mice. At the steady state, as well as following infection on days 1, 3, and 5, the number of inflammatory monocytes, neutrophils, NK cells, CD4^{+} T cells, CD8^{+} T cells, and B cells present in the blood were unaffected in the absence of Ccr5 (Figure 2A). Since viral infections induce innate immune mediators indicative of the antiviral response, we next measured several proinflammatory factors known to be produced following infection, such as interferon-stimulated proteins (Ccl2, Cxcl9, and Cxcl10), immunosuppressive cytokine IL-10, and the Ccr5 ligands (Ccl4 and Ccl5). Levels of Ccl4 and Ccl5 were the only differences observed between LGTV-infected WT and *Ccr5*$^{-/-}$ mice (Figure 2B). Significantly higher levels of Ccl5 were measured at the steady state in the Ccr5-deficient mice, and following infection, Ccl4 and Ccl5 were three- to six-fold higher than WT levels. This is consistent with previous studies showing that the loss of Ccr5 results in the inability to bind and degrade these ligands (15, 30, 31). As all leukocyte numbers, as well as cytokine and chemokine levels (apart from the cognate ligands) were unaltered, the increased susceptibility observed in the Ccr5-deficient mice is not a direct result of a deficit in leukocyte numbers in the periphery or differences in the initial host cytokine response to infection.

Ccr5 results in impaired T and NK cell trafficking to the CNS

Given that no differences in peripheral viral loads, leukocyte numbers, or cytokine production was observed following LGTV infection, we next assessed whether the accumulation of lymphocytes into the CNS was altered given the role of Ccr5 in leukocyte migration. Leukocytes were isolated from brains of WT and Ccr5-deficient mice on days 8 and 12 post infection and analyzed by flow cytometry. On day 8 post infection, after virus has entered the CNS, we found a significant reduction of CD4^{+} T cells (~46%), CD8^{+} T cells (~49%) and NK cells (~53%) in the brains of *Ccr5*$^{-/-}$ mice compared to WT mice (Figure 3A–F). This delay coincided with weight loss (Figure 1B) and disease symptom onset, and transient since differences were no longer apparent by day 12 post infection, with CD4^{+}, CD8^{+} T cells, and NK cell numbers returning to those nearly identical to WT mice. To further evaluate the nature of the differences in T cell migration into the CNS, we conducted immunohistochemical analyses on the brain tissue of WT and Ccr5-deficient mice. As shown in Figure 3G, the number of CD3^{+} T cells was greatly reduced in the brains of Ccr5-deficient mice on day 8 post infection, which was observed in all regions in the brain, with representative images shown for the cerebellum. These differences were no longer observed on day 12, which showed similar staining for CD3^{+} T cells between the strains, confirming the flow cytometry results.

Enhanced neutrophil recruitment in the absence of Ccr5 leads to neuropathology

We next evaluated monocytes and neutrophils within the CNS as these cell populations have been shown to accumulate in the CNS during WNV and JEV infection (13, 28, 32). In the absence of Ccr5, the number of inflammatory monocytes was similar between WT and Ccr5-deficient mice (Figure 4A and B). Consistent with this result, no significant differences were observed in the protein levels of Ccl2 and Ccl7, known chemoattractants for inflammatory monocytes (Figure 4C and D) (33). Evaluation of neutrophils in the infected CNS revealed similar numbers on day 8 post infection, but by day 12 post infection, there was a 2–3 fold increase in the total number of neutrophils in the brains of *Ccr5*$^{-/-}$ mice

(Figure 4E and F). Evaluation of neutrophil attracting chemokines, Cxcl1 and Cxcl2, within the CNS also showed significantly elevated levels in the CNS in the absence of Ccr5 specifically on day 12 post infection (Fig. 4G and H). To further characterize neutrophil infiltration into the CNS, immunohistochemistry was performed on brain slices from WT and Ccr5-deficient mice on days 8 and 12 post infection. Staining for myeloperoxidase (MPO), an enzyme abundantly expressed by neutrophils, was similar on day 8 post infection between the two strains but was markedly increased in the brains of Ccr5-deficient mice on day 12, including the meninges and the cortex as shown in Figure 5A. Taken together, these data confirm that neutrophil infiltration into the brain is increased in the absence of Ccr5 during LGTV infection during the late phase of infection.

Previous studies have shown that flaviviruses, including LGTV, can induce apoptosis of infected cells *in vitro*, suggesting a mechanism by which damage to neurons within the CNS can occur (34–37). Given that the *Ccr5*$^{-/-}$ mice have increased viral replication within the CNS, we hypothesized that this may lead to a significant increase in apoptotic cells. To test this, we evaluated WT and *Ccr5*$^{-/-}$ CNS tissue for apoptosis using TUNEL staining. On day 8 post infection, when viral loads are similar between WT and *Ccr5*$^{-/-}$ mice, the number of apoptotic cells was nearly identical between both strains. By day 12 post infection, there was a significant increase in the number of apoptotic cells in the CNS of Ccr5-deficient mice, which we observed in various regions of the CNS, including the cortex and meninges as shown in Figure 5B.

Survival during LGTV encephalitis involves promoting T cells and reducing neutrophils into the CNS

Our data thus far suggest that Ccr5 may regulate the efficient migration of effector lymphocytes (T and NK cells) into the CNS. In the absence of Ccr5, the delayed migration of these cells likely results in increased viral replication that coincides with aberrant production of neutrophil-associated chemokines, leading to increased neutrophil influx and associated immunopathology. Due to the known antiviral role of T cells in neuroprotection, and the known role of neutrophils in neuropathology, we hypothesized that both T cells and neutrophils may be involved in the increased mortality observed in the *Ccr5*$^{-/-}$ mice (38–41). To determine the relative contribution of T cells to survival, we adoptively transferred T cells isolated from the spleens of LGTV-infected WT or *Ccr5*$^{-/-}$ donors into LGTV-infected *Ccr5*$^{-/-}$ recipients 5 days post infection and evaluated survival (Figure 6A). LGTV-infected *Ccr5*$^{-/-}$ recipients receiving WT T cells showed a significant improvement in survival compared to *Ccr5*$^{-/-}$ recipients receiving *Ccr5*$^{-/-}$ T cells ($p<0.05$; Figure 6B). This increase in survival was indeed accompanied by an increase in CD3^{+} T cells accumulating in the CNS of *Ccr5*$^{-/-}$ recipients receiving WT T cells, in comparison to *Ccr5*$^{-/-}$ recipients receiving *Ccr5*$^{-/-}$ T cells (Figure 6C). Although CCR5-expressing T cells appeared to provide a survival benefit, protection was not completely restored to WT levels, suggesting that other factors are important for Ccr5-mediated survival.

We next evaluated the impact of neutrophil migration into the CNS. Because neutrophil numbers in the CNS were nearly identical between WT and *Ccr5*$^{-/-}$ mice on day 8 post infection, and differed only on day 12 post infection, we depleted neutrophils starting on day

8 post infection, after the onset of weight loss and symptoms. To deplete neutrophils, we treated LGTV-infected *Ccr5*$^{-/-}$ mice with the monoclonal antibody Ly6G (clone 1A8) or isotype control on days 8, 10, and 12 post infection. A ~99% depletion of neutrophils was achieved that lasted 48 hours as previously shown (42–44). While weight loss was observed in both groups of mice starting on day 7 post infection, this was significantly less pronounced in the neutrophil-depleted mice on days 10, 11, and 12 post infection compared to isotype control-treated mice (Figure 6D). Accordingly, 1A8-treated mice exhibited fewer signs of illness and showed improved survival outcome, with a survival rate of 75% among 1A8-treated mice vs. 35% for the isotype control-treated mice (Figure 6E; $p<0.05$). Interestingly, evaluation of the brain tissue showed a ~12 fold decrease in viral titer in the neutropenic mice ($p=0.034$) compared to isotype control-treated mice (Figure 6F).

To further characterize this phenotype, we conducted immunohistochemical analysis of the mouse brains of 1A8- or isotype control-treated mice. Consistent with the flow cytometry data, staining with MPO showed no reactivity in the 1A8-treated mouse brains in comparison to isotype control-treated mice, where prominent neutrophil staining was observed (Figure 6G). To determine the extent of neuropathology in the brain, a TUNEL assay was performed. Staining revealed that the number of apoptotic cells within the brain was lower in the neutrophil-depleted mice compared to controls, suggesting that the presence of neutrophils in the CNS is damaging (Figure 6H–J, left panels). Apoptotic cells were observed in various regions within the CNS, including the meninges (Figure 6H), hippocampus (Figure 6I), and cortex (Figure 6J). We next determined whether regions of apoptosis were also regions of viral replication. To test this, serial brain sections of isotype control and 1A8-treated mice were also stained for LGTV. We found that LGTV-infected cells were in close proximity to TUNEL positive cells in various parts of the CNS (Figure 6H–J, right panels). In neutrophil-depleted mice, there were fewer LGTV-infected cells, consistent with the decrease in viral titers, which correlated with an overall decrease in apoptosis within the tissue. Together, our data suggest that neutrophils promote viral replication within the CNS, drive apoptosis, and negatively impact survival.

DISCUSSION

One of the hallmarks of viral encephalitis is the influx of leukocytes into the CNS to clear virus and aid recovery. This process can also cause collateral damage, particularly in delicate tissues such as the brain by causing the destruction of irreparable neurons and glial cells. In this manuscript, we demonstrate that Ccr5 regulates this balance by coordinating the efficient migration of effector T cells and NK cells into the CNS. In the absence of Ccr5, virus is inefficiently controlled at the early time points due to a lag in lymphocyte migration. This tips the balance towards greater virus replication, causing an excess production of chemokines, the subsequent infiltration of neutrophils, and induction of neuroimmunopathology, an unanticipated phenotype that has not been described to occur in models of WNV or JEV. Given these results in mice, our data have implications for individuals deficient for CCR5, who will likely be at higher risk of developing symptomatic TBEV infection. CCR5-deficient cohorts include individuals with genetically-altered CCR5 function, including *CCR5Δ32* homozygotes found in ~1% of individuals of European decent (45), as well as individuals prescribed FDA-approved CCR5 antagonist Maraviroc for the

treatment of HIV infection and other chronic inflammatory conditions (46, 47). In fact, several human cohort studies have investigated the association of *CCR5Δ32* and TBEV. Two studies have shown that the frequency of *CCR5Δ32* homozygotes was elevated among TBE patients, while a third study was unable to find an association (48–50). Our studies with LGTV in mice support a protective role for CCR5 during tick-borne flavivirus infections.

Since Ccr5 is expressed primarily on activated subsets of T cells, a large percentage of the infiltrating, virus-specific T cells within the CNS are likely to express this receptor. A previous study has shown that a small percentage of T cells express Ccr5 at the steady state and that expression increases 10-fold following inflammation (10, 51). In humans, CCR5 expression has been to shown to increase significantly following Dengue virus infection (51). Functionally, the infiltration of activated $CD4^+$ and $CD8^+$ T cells into the CNS has been shown to be critical for controlling viral replication in the context of WNV and JEV. In these studies, $CD8^+$ T cells are strongly correlated with increased survival through perforin- and Fas-mediated mechanisms (40, 52). Similarly, $CD4^+$ T cells are critical for survival since the absence of these cells in mice resulted in persistent infection in the CNS, ultimately leading to uniform mortality (53). CCR5 is expressed on a large proportion of T cells found in the CSF of TBEV-infected individuals (54). However the role of T cells during TBEV infection is unclear; in the context of infection with the Central European subtype, T cells appear to be immunopathogenic since CD8-deficient mice or SCID mice have a significant survival advantage (41). The data generated in this manuscript do not support a pathogenic role for T cells but rather suggest that T cells within the CNS promote survival, consistent with data generated in WNV and JEV infection models.

The role of neutrophils during flavivirus infections is currently poorly defined. However, the presence of neutrophils into the CNS has been demonstrated in numerous models of flavivirus infections, including MVEV, TBEV, and WNV (28, 55, 56). Our data suggest that neutrophils promote viral replication and pathology by shuttling virus into the CNS. Support for this model comes from our data showing that increased neutrophils in the CNS correlate with greater viral replication and apoptosis in the brain tissue, a phenotype that is reversed following neutrophil depletion. This model is supported by another published report showing that neutrophils are cellular targets for infection with TBEV and also undergo apoptosis following infection (35). Similarly, neutrophils are readily infected *ex vivo* by the related virus, WNV, and may serve as an important reservoir of virus replication *in vivo* (57). Furthermore, a recent study has shown that neutrophils have a detrimental role in an ocular model of HSV-1 infection, where neutrophils serve as a conduit for virus replication (58). Thus, our data align with the idea that neutrophils contribute to pathology through their function as a reservoir for viruses and presumably through immune-mediated mechanisms.

One limitation of our study is that we do not know which cells within the CNS are undergoing apoptosis. Within the CNS, neurons are the primary target for infection by TBEV and undergo apoptosis (59–62). While astrocytes can also become infected, these cells appear to be primarily involved in cytokine production and do not undergo morphological changes or apoptosis (63, 64). We do show that LGTV antigen co-localized to areas of apoptotic cells, and based on previous literature, these infected cells may be primarily neurons and/or neutrophils (35, 59–62). Our study also does not address the

mechanism by which neutrophils function within the CNS. While the CNS injury observed in the current study may be directly caused by viral infection, neuronal destruction has been attributed to an indirect effect of infiltrating immune cells and production of inflammatory cytokines (4, 59, 65). Therefore neutrophil-mediated indirect destruction of cells in the brain cannot be excluded. Recent literature has shown that neutrophils promote Alzheimer's disease-like pathology in the brain through the release of neutrophil extracellular traps (NETs) (66). Therefore neutrophils may be further mediating brain damage through the release of NETs and/or reactive oxygen/nitrogen intermediates during tick-borne flavivirus infection. From a translational standpoint, our data suggest that neutrophil depletion during symptom onset would promote recovery following TBEV infection in humans and, in fact, may be beneficial since neutrophils in the CNS, viral load, and damage are positively correlated and intimately coupled. Since no specific antivirals or immunomodulatory therapies exist for the treatment of individuals infected with any neurotropic flavivirus, our findings provide novel directions with regards to immunomodulators of the host response, which are greatly needed.

ACKNOWLEDGEMENTS

We would like to thank the Flow Cytometry Shared Resource Facility, mouse facility, and Microscopy CORE at Icahn School of Medicine at Mount Sinai for their technical assistance. This work was funded by the NIAID R01AI108715 and supported in part by the NIH Research Training Award T32AI007647 and NIAID F31AI110071.

[1]This work was funded by the NIAID R01AI108715 and supported in part by the Division of Intramural Research, NIAID, NIH. S.V.B. was supported in part by NIH Research Training Award T32AI007647 and NIAID F31AI110071.

3Abbreviations used in this paper

LGTV	Langat virus
WT	wild type
FFU	focus forming unit
p.i.	post infection.

REFERENCES

1. Donoso-Mantke, O.; K.L.S.; Ruzek, D. InTechOpen. 1st ed.. 2011. Tick-Borne Encephalitis Virus: A General Overview.
2. Gritsun TS, Lashkevich VA, Gould EA. Tick-borne encephalitis. Antiviral research. 2003; 57:129–146. [PubMed: 12615309]
3. Suss J. Tick-borne encephalitis in Europe and beyond--the epidemiological situation as of 2007. Euro surveillance : bulletin Europeen sur les maladies transmissibles = European communicable disease bulletin. 2008; 13
4. Ruzek D, Dobler G, Donoso Mantke O. Tick-borne encephalitis: pathogenesis and clinical implications. Travel medicine and infectious disease. 2010; 8:223–232. [PubMed: 20970725]
5. Bogovic P, Strle F. Tick-borne encephalitis: A review of epidemiology, clinical characteristics, and management. World journal of clinical cases. 2015; 3:430–441. [PubMed: 25984517]
6. European, C. f. D. C. European Center for Disease Prevention and Control. 2012. Epidemiological situation of tick-borne enceohalitis in the EU/EFTA countries.

7. Dobler G. Zoonotic tick-borne flaviviruses. Veterinary microbiology. 2010; 140:221–228. [PubMed: 19765917]
8. Michlmayr D, Lim JK. Chemokine receptors as important regulators of pathogenesis during arboviral encephalitis. Frontiers in cellular neuroscience. 2014; 8:264. [PubMed: 25324719]
9. Bardina SV, Lim JK. The role of chemokines in the pathogenesis of neurotropic flaviviruses. Immunologic research. 2012; 54:121–132. [PubMed: 22547394]
10. Mack M, Cihak J, Simonis C, Luckow B, Proudfoot AE, Plachy J, Bruhl H, Frink M, Anders HJ, Vielhauer V, Pfirstinger J, Stangassinger M, Schlondorff D. Expression and characterization of the chemokine receptors CCR2 and CCR5 in mice. Journal of immunology (Baltimore, Md : 1950). 2001; 166:4697–4704.
11. Glass WG, McDermott DH, Lim JK, Lekhong S, Yu SF, Frank WA, Pape J, Cheshier RC, Murphy PM. CCR5 deficiency increases risk of symptomatic West Nile virus infection. The Journal of experimental medicine. 2006; 203:35–40. [PubMed: 16418398]
12. Lim JK, Glass WG, McDermott DH, Murphy PM. CCR5: no longer a “good for nothing” gene--chemokine control of West Nile virus infection. Trends in immunology. 2006; 27:308–312. [PubMed: 16753343]
13. Larena M, Regner M, Lobigs M. The chemokine receptor CCR5, a therapeutic target for HIV/AIDS antagonists, is critical for recovery in a mouse model of Japanese encephalitis. PloS one. 2012; 7:e44834. [PubMed: 23028638]
14. Huffnagle GB, McNeil LK, McDonald RA, Murphy JW, Toews GB, Maeda N, Kuziel WA. Cutting edge: Role of C-C chemokine receptor 5 in organ-specific and innate immunity to Cryptococcus neoformans. Journal of immunology (Baltimore, Md : 1950). 1999; 163:4642–4646.
15. Thapa M, Kuziel WA, Carr DJ. Susceptibility of CCR5-deficient mice to genital herpes simplex virus type 2 is linked to NK cell mobilization. Journal of virology. 2007; 81:3704–3713. [PubMed: 17267483]
16. Durrant DM, Daniels BP, Pasieka T, Dorsey D, Klein RS. CCR5 limits cortical viral loads during West Nile virus infection of the central nervous system. Journal of neuroinflammation. 2015; 12:233. [PubMed: 26667390]
17. Glass WG, Lim JK, Cholera R, Pletnev AG, Gao JL, Murphy PM. Chemokine receptor CCR5 promotes leukocyte trafficking to the brain and survival in West Nile virus infection. The Journal of experimental medicine. 2005; 202:1087–1098. [PubMed: 16230476]
18. Lim JK, Louie CY, Glaser C, Jean C, Johnson B, Johnson H, McDermott DH, Murphy PM. Genetic deficiency of chemokine receptor CCR5 is a strong risk factor for symptomatic West Nile virus infection: a meta-analysis of 4 cohorts in the US epidemic. The Journal of infectious diseases. 2008; 197:262–265. [PubMed: 18179388]
19. Lim JK, McDermott DH, Lisco A, Foster GA, Krysztof D, Follmann D, Stramer SL, Murphy PM. CCR5 deficiency is a risk factor for early clinical manifestations of West Nile virus infection but not for viral transmission. The Journal of infectious diseases. 2010; 201:178–185. [PubMed: 20025530]
20. Campbell GL, Hills SL, Fischer M, Jacobson JA, Hoke CH, Hombach JM, Marfin AA, Solomon T, Tsai TF, Tsu VD, Ginsburg AS. Estimated global incidence of Japanese encephalitis: a systematic review. Bulletin of the World Health Organization. 2011; 89:766–774. 774a–774e. [PubMed: 22084515]
21. Mandl CW, Iacono-Connors L, Wallner G, Holzmann H, Kunz C, Heinz FX. Sequence of the genes encoding the structural proteins of the low-virulence tick-borne flaviviruses Langat TP21 and Yelantsev. Virology. 1991; 185:891–895. [PubMed: 1720591]
22. Muhd Radzi SF, Ruckert C, Sam SS, Teoh BT, Jee PF, Phoon WH, Abubakar S, Zandi K. Detection of Langat virus by TaqMan real-time one-step qRT-PCR method. Scientific reports. 2015; 5:14007. [PubMed: 26360297]
23. Rumyantsev AA, Murphy BR, Pletnev AG. A tick-borne Langat virus mutant that is temperature sensitive and host range restricted in neuroblastoma cells and lacks neuroinvasiveness for immunodeficient mice. Journal of virology. 2006; 80:1427–1439. [PubMed: 16415020]

24. Pletnev AG, Men R. Attenuation of the Langat tick-borne flavivirus by chimerization with mosquito-borne flavivirus dengue type 4. Proceedings of the National Academy of Sciences of the United States of America. 1998; 95:1746–1751. [PubMed: 9465088]
25. Pletnev AG. Infectious cDNA clone of attenuated Langat tick-borne flavivirus (strain E5) and a 3' deletion mutant constructed from it exhibit decreased neuroinvasiveness in immunodeficient mice. Virology. 2001; 282:288–300. [PubMed: 11289811]
26. Gritsun TS, Desai A, Gould EA. The degree of attenuation of tick-borne encephalitis virus depends on the cumulative effects of point mutations. The Journal of general virology. 2001; 82:1667–1675. [PubMed: 11413378]
27. Heaton NS, Langlois RA, Sachs D, Lim JK, Palese P, tenOever BR. Long-term survival of influenza virus infected club cells drives immunopathology. The Journal of experimental medicine. 2014; 211:1707–1714. [PubMed: 25135297]
28. Bardina SV, Michlmayr D, Hoffman KW, Obara CJ, Sum J, Charo IF, Lu W, Pletnev AG, Lim JK. Differential Roles of Chemokines CCL2 and CCL7 in Monocytosis and Leukocyte Migration during West Nile Virus Infection. Journal of immunology (Baltimore, Md : 1950). 2015; 195:4306–4318.
29. Michlmayr D, McKimmie CS, Pingen M, Haxton B, Mansfield K, Johnson N, Fooks AR, Graham GJ. Defining the chemokine basis for leukocyte recruitment during viral encephalitis. Journal of virology. 2014; 88:9553–9567. [PubMed: 24899190]
30. Carr DJ, Ash J, Lane TE, Kuziel WA. Abnormal immune response of CCR5-deficient mice to ocular infection with herpes simplex virus type 1. The Journal of general virology. 2006; 87:489–499. [PubMed: 16476970]
31. Schuh JM, Blease K, Hogaboam CM. The role of CC chemokine receptor 5 (CCR5) and RANTES/CCL5 during chronic fungal asthma in mice. FASEB journal : official publication of the Federation of American Societies for Experimental Biology. 2002; 16:228–230. [PubMed: 11744622]
32. Lim JK, Murphy PM. Chemokine control of West Nile virus infection. Experimental cell research. 2011; 317:569–574. [PubMed: 21376172]
33. Shi C, Jia T, Mendez-Ferrer S, Hohl TM, Serbina NV, Lipuma L, Leiner I, Li MO, Frenette PS, Pamer EG. Bone marrow mesenchymal stem and progenitor cells induce monocyte emigration in response to circulating toll-like receptor ligands. Immunity. 2011; 34:590–601. [PubMed: 21458307]
34. Prikhod'ko GG, Prikhod'ko EA, Cohen JI, Pletnev AG. Infection with Langat Flavivirus or expression of the envelope protein induces apoptotic cell death. Virology. 2001; 286:328–335. [PubMed: 11485400]
35. Plekhova NG, Somova LM, Lyapun IN, Krylova NV, Leonova GN. Neutrophil apoptosis induction by tick-borne encephalitis virus. Bulletin of experimental biology and medicine. 2012; 153:105–108. [PubMed: 22808506]
36. Liao CL, Lin YL, Wang JJ, Huang YL, Yeh CT, Ma SH, Chen LK. Effect of enforced expression of human bcl-2 on Japanese encephalitis virus-induced apoptosis in cultured cells. Journal of virology. 1997; 71:5963–5971. [PubMed: 9223486]
37. Shrestha B, Gottlieb D, Diamond MS. Infection and injury of neurons by West Nile encephalitis virus. Journal of virology. 2003; 77:13203–13213. [PubMed: 14645577]
38. Herz J, Sabellek P, Lane TE, Gunzer M, Hermann DM, Doeppner TR. Role of Neutrophils in Exacerbation of Brain Injury After Focal Cerebral Ischemia in Hyperlipidemic Mice. Stroke; a journal of cerebral circulation. 2015; 46:2916–2925.
39. Jickling GC, Liu D, Ander BP, Stamova B, Zhan X, Sharp FR. Targeting neutrophils in ischemic stroke: translational insights from experimental studies. Journal of cerebral blood flow and metabolism : official journal of the International Society of Cerebral Blood Flow and Metabolism. 2015; 35:888–901.
40. Shrestha B, Samuel MA, Diamond MS. CD8+ T cells require perforin to clear West Nile virus from infected neurons. Journal of virology. 2006; 80:119–129. [PubMed: 16352536]

41. Ruzek D, Salat J, Palus M, Gritsun TS, Gould EA, Dykova I, Skallova A, Jelinek J, Kopecky J, Grubhoffer L. CD8+ T-cells mediate immunopathology in tick-borne encephalitis. Virology. 2009; 384:1–6. [PubMed: 19070884]
42. Carr KD, Sieve AN, Indramohan M, Break TJ, Lee S, Berg RE. Specific depletion reveals a novel role for neutrophil-mediated protection in the liver during Listeria monocytogenes infection. European journal of immunology. 2011; 41:2666–2676. [PubMed: 21660934]
43. Daley JM, Thomay AA, Connolly MD, Reichner JS, Albina JE. Use of Ly6G-specific monoclonal antibody to deplete neutrophils in mice. Journal of leukocyte biology. 2008; 83:64–70. [PubMed: 17884993]
44. Bugl S, Wirths S, Radsak MP, Schild H, Stein P, Andre MC, Muller MR, Malenke E, Wiesner T, Marklin M, Frick JS, Handgretinger R, Rammensee HG, Kanz L, Kopp HG. Steady-state neutrophil homeostasis is dependent on TLR4/TRIF signaling. Blood. 2013; 121:723–733. [PubMed: 23223360]
45. Galvani AP, Novembre J. The evolutionary history of the CCR5-Delta32 HIV-resistance mutation. Microbes and infection / Institut Pasteur. 2005; 7:302–309. [PubMed: 15715976]
46. Gilliam BL, Riedel DJ, Redfield RR. Clinical use of CCR5 inhibitors in HIV and beyond. Journal of translational medicine. 2011; 9(Suppl 1):S9. [PubMed: 21284908]
47. Liu T, Weng Z, Dong X, Hu Y. Recent advances in the development of small-molecule CCR5 inhibitors for HIV. Mini reviews in medicinal chemistry. 2010; 10:1277–1292. [PubMed: 20854256]
48. Hladik F, Liu H, Speelmon E, Livingston-Rosanoff D, Wilson S, Sakchalathorn P, Hwangbo Y, Greene B, Zhu T, McElrath MJ. Combined effect of CCR5-Delta32 heterozygosity and the CCR5 promoter polymorphism -2459 A/G on CCR5 expression and resistance to human immunodeficiency virus type 1 transmission. Journal of virology. 2005; 79:11677–11684. [PubMed: 16140745]
49. Weber E, Finsterbusch K, Lindquist R, Nair S, Lienenklaus S, Gekara NO, Janik D, Weiss S, Kalinke U, Overby AK, Kroger A. Type I interferon protects mice from fatal neurotropic infection with Langat virus by systemic and local antiviral responses. Journal of virology. 2014; 88:12202–12212. [PubMed: 25122777]
50. Carrington M, Kissner T, Gerrard B, Ivanov S, O'Brien SJ, Dean M. Novel alleles of the chemokine-receptor gene CCR5. American journal of human genetics. 1997; 61:1261–1267. [PubMed: 9399903]
51. de-Oliveira-Pinto LM, Marinho CF, Povoa TF, de Azeredo EL, de Souza LA, Barbosa LD, Motta-Castro AR, Alves AM, Avila CA, de Souza LJ, da Cunha RV, Damasco PV, Paes MV, Kubelka CF. Regulation of inflammatory chemokine receptors on blood T cells associated to the circulating versus liver chemokines in dengue fever. PloS one. 2012; 7:e38527. [PubMed: 22815692]
52. Shrestha B, Diamond MS. Fas ligand interactions contribute to CD8+ T-cell-mediated control of West Nile virus infection in the central nervous system. Journal of virology. 2007; 81:11749–11757. [PubMed: 17804505]
53. Sitati EM, Diamond MS. CD4+ T-cell responses are required for clearance of West Nile virus from the central nervous system. Journal of virology. 2006; 80:12060–12069. [PubMed: 17035323]
54. Grygorczuk S, Osada J, Parczewski M, Moniuszko A, Swierzbinska R, Kondrusik M, Czupryna P, Dunaj J, Dabrowska M, Pancewicz S. The expression of the chemokine receptor CCR5 in tick-borne encephalitis. Journal of neuroinflammation. 2016; 13:45. [PubMed: 26906062]
55. Andrews DM, Matthews VB, Sammels LM, Carrello AC, McMinn PC. The severity of murray valley encephalitis in mice is linked to neutrophil infiltration and inducible nitric oxide synthase activity in the central nervous system. Journal of virology. 1999; 73:8781–8790. [PubMed: 10482632]
56. Tonteri E, Kipar A, Voutilainen L, Vene S, Vaheri A, Vapalahti O, Lundkvist A. The three subtypes of tick-borne encephalitis virus induce encephalitis in a natural host, the bank vole (Myodes glareolus). PloS one. 2013; 8:e81214. [PubMed: 24349041]
57. Bai F, Kong KF, Dai J, Qian F, Zhang L, Brown CR, Fikrig E, Montgomery RR. A paradoxical role for neutrophils in the pathogenesis of West Nile virus. The Journal of infectious diseases. 2010; 202:1804–1812. [PubMed: 21050124]

58. Royer DJ, Zheng M, Conrady CD, Carr DJ. Granulocytes in Ocular HSV-1 Infection: Opposing Roles of Mast Cells and Neutrophils. Investigative ophthalmology & visual science. 2015; 56:3763–3775. [PubMed: 26066745]

59. Ruzek D, Vancova M, Tesarova M, Ahantarig A, Kopecky J, Grubhoffer L. Morphological changes in human neural cells following tick-borne encephalitis virus infection. The Journal of general virology. 2009; 90:1649–1658. [PubMed: 19264624]

60. Bily T, Palus M, Eyer L, Elsterova J, Vancova M, Ruzek D. Electron Tomography Analysis of Tick-Borne Encephalitis Virus Infection in Human Neurons. Scientific reports. 2015; 5:10745. [PubMed: 26073783]

61. Hirano M, Yoshii K, Sakai M, Hasebe R, Ichii O, Kariwa H. Tick-borne flaviviruses alter membrane structure and replicate in dendrites of primary mouse neuronal cultures. The Journal of general virology. 2014; 95:849–861. [PubMed: 24394700]

62. Gelpi E, Preusser M, Garzuly F, Holzmann H, Heinz FX, Budka H. Visualization of Central European tick-borne encephalitis infection in fatal human cases. Journal of neuropathology and experimental neurology. 2005; 64:506–512. [PubMed: 15977642]

63. Potokar M, Korva M, Jorgacevski J, Avsic-Zupanc T, Zorec R. Tick-borne encephalitis virus infects rat astrocytes but does not affect their viability. PloS one. 2014; 9:e86219. [PubMed: 24465969]

64. Palus M, Bily T, Elsterova J, Langhansova H, Salat J, Vancova M, Ruzek D. Infection and injury of human astrocytes by tick-borne encephalitis virus. The Journal of general virology. 2014; 95:2411–2426. [PubMed: 25000960]

65. Hayasaka D, Nagata N, Fujii Y, Hasegawa H, Sata T, Suzuki R, Gould EA, Takashima I, Koike S. Mortality following peripheral infection with tick-borne encephalitis virus results from a combination of central nervous system pathology, systemic inflammatory and stress responses. Virology. 2009; 390:139–150. [PubMed: 19467556]

66. Zenaro E, Pietronigro E, Della Bianca V, Piacentino G, Marongiu L, Budui S, Turano E, Rossi B, Angiari S, Dusi S, Montresor A, Carlucci T, Nani S, Tosadori G, Calciano L, Catalucci D, Berton G, Bonetti B, Constantin G. Neutrophils promote Alzheimer's disease-like pathology and cognitive decline via LFA-1 integrin. Nature medicine. 2015; 21:880–886.

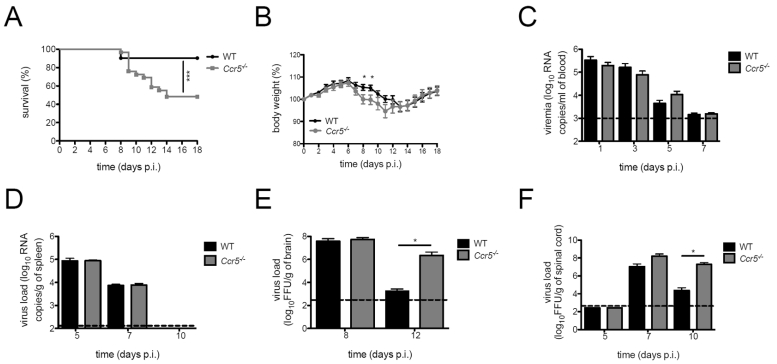

Figure 1. Ccr5 is critical for survival and viral clearance in the CNS during LGTV infection

(A) Kaplan-Meier survival analysis of LGTV-infected WT (black circles) and *Ccr5*$^{-/-}$ (grey squares) mice. **(B)** Body weight was measured for LGTV-infected WT and *Ccr5*$^{-/-}$ mice. All data shown (A–B) are pooled from three independent experiments (31 WT mice and 32 *Ccr5*$^{-/-}$ mice). Viral titers were quantified in **(C)** the blood and **(D)** spleen by qRT-PCR, and in **(E)** the brain and **(F)** spinal cord by FFU assay. Dotted lines indicate the limit of detection. All data (C–F) are shown as mean ± SD for 3–8 mice per genotype and time point from two independent experiments. * $p<0.05$ and *** $p<0.001$.

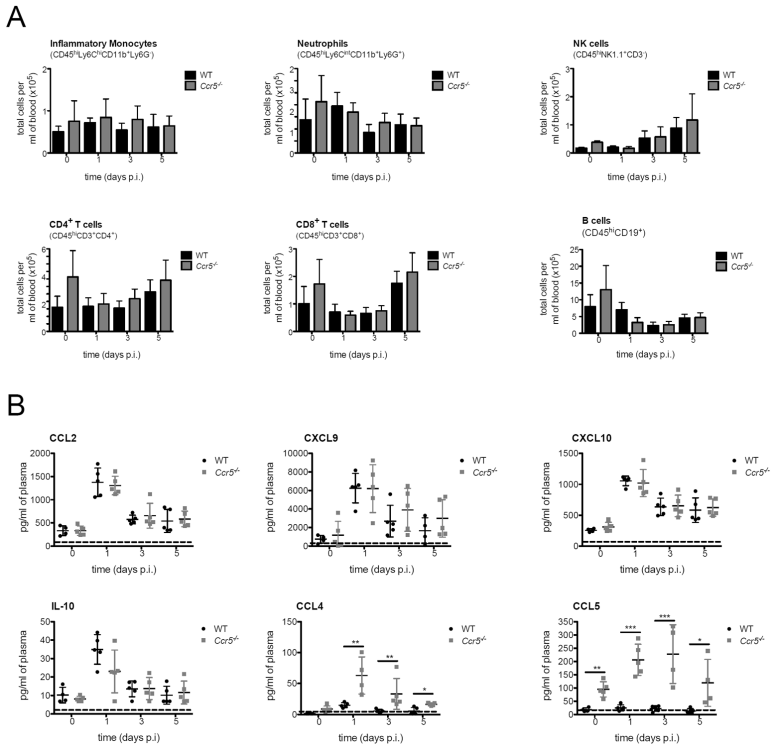

Figure 2. Peripheral leukocytes and inflammatory cytokine production following LGTV infection

(A) Total cell numbers of monocytes ($CD45^{hi}Ly6C^{hi}CD11b^{+}Ly6G^{-}$), neutrophils ($CD45^{hi}Ly6C^{int}CD11b^{+}Ly6G^{+}$), NK cells ($CD45^{hi}NK1.1^{+}CD3^{-}$), $CD4^{+}$ T cells ($CD45^{hi}CD3^{+}$ $CD4^{+}$), $CD8^{+}$ T cells ($CD45^{hi}CD3^{+}CD8^{+}$) and B cells ($CD45^{hi}CD19^{+}$) were assessed by flow cytometry from the blood of WT and *Ccr5*$^{-/-}$ mice on days 0, 1, 3, and 5 post infection. Cells were gated on live singlet $CD45^{hi}$ cells. **(B)** Levels of Ccl2, Cxcl9, Cxcl10, IL-10, Ccl4, and Ccl5 in the blood of WT and *Ccr5*$^{-/-}$ mice were measured by multiplex ELISA. The dotted line represents the assay limit of detection. All data are shown as mean ± SD for 4–11 mice per genotype and time point from three independent experiments. * $p<0.05$, ** $p<0.01$ and *** $p<0.001$.

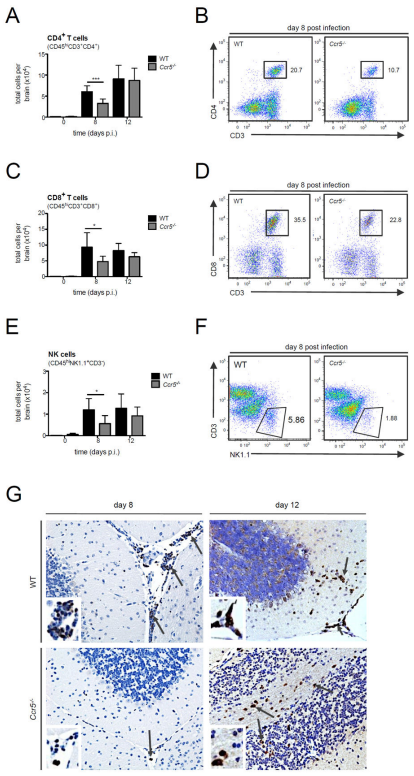

Figure 3. T and NK cell infiltration into the CNS is impaired in the absence of Ccr5 during LGTV infection

The total number of **(A)** $CD4^+$ T cells ($CD45^{hi}CD3^+CD4^+$), **(C)** $CD8^+$ T cells ($CD45^{hi}CD3^+CD8^+$) and **(E)** NK cells ($CD45^{hi}NK1.1^+CD3^-$) were assessed by flow cytometry in the brains of WT and *Ccr5*$^{-/-}$ mice. Data are shown as mean ±SD for 3–9 mice per genotype and time point from two independent experiments. Representative flow cytometry plots on day 8 post infection for **(B)** $CD4^+$ T cells, **(D)** $CD8^+$ T cells, and **(F)** NK cells are displayed. Cells were gated on live singlet $CD45^{hi}$ cells. **(G)** Paraffin-embedded brain sections from WT and *Ccr5*$^{-/-}$ mice were stained for CD3, and positive cells (brown cells, indicated by arrows) are shown within the cerebellum of LGTV-infected mice on days 8 and 12 post infection for 3-5 mice per genotype from two independent experiments. Representative images are shown at 20× magnification. * $p<0.05$ and *** $p<0.001$.

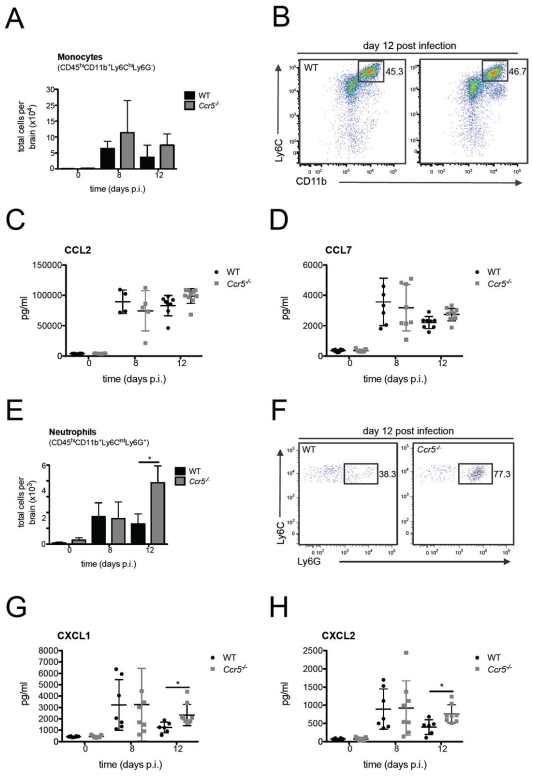

Figure 4. Neutrophil numbers are increased in the CNS in the absence of Ccr5

The total number of **(A)** monocytes ($CD45^{hi}CD11b^{+}Ly6C^{hi}Ly6G^{-}$) and **(E)** neutrophils ($CD45^{hi}CD11b^{+}Ly6C^{int}Ly6G^{+}$) in the brain of uninfected and LGTV-infected WT and *Ccr5*$^{-/-}$ mice on days 8 and 12 post infection were assessed by flow cytometry. Representative flow cytometry plots from day 12 post infection are shown for **(B)** monocytes and **(F)** neutrophils. Cells were gated on live singlet $CD45^{hi}$ cells. Neutrophils were additionally gated on $CD11b^{+}$ and $Ly6C^{int}$ cells. The protein levels of monocyte chemoattractants **(C)** Ccl2 and, **(D)** Ccl7, and neutrophil chemoattractants **(G)** Cxcl1 and **(H)** Cxcl2 were measured by multiplex ELISA. All data are shown as mean ± SD with 4–10 mice per time point and genotype and were pooled from two independent experiments. A Student's *t*-test was performed for statistical analysis with $*p<0.05$.

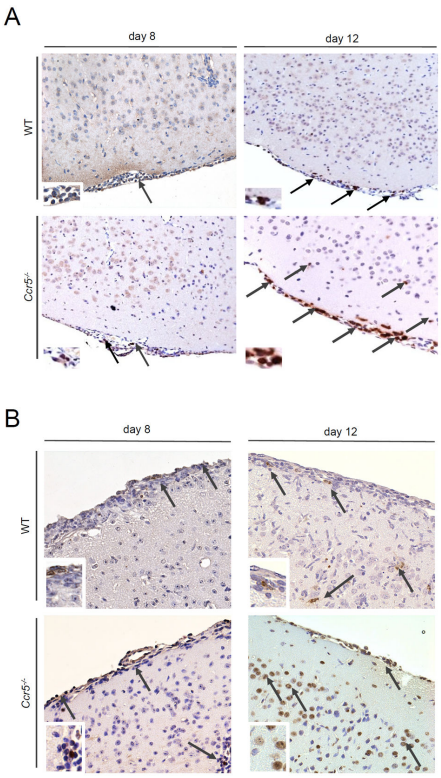

Figure 5. Enhanced neutrophil accumulation in the brain is accompanied by increased apoptosis in *Ccr5*$^{-/-}$ mice during LGTV-induced encephalitis

Paraffin-embedded brain sections of LGTV-infected mice on days 8 and 12 post infection were stained for **(A)** myeloperoxidase and **(B)** apoptosis using TUNEL assay for 3-5 mice per genotype and condition from two independent experiments. Arrows indicate the positive cells (brown staining) within the cortex and meninges. Representative images are shown at a magnification of 20×.

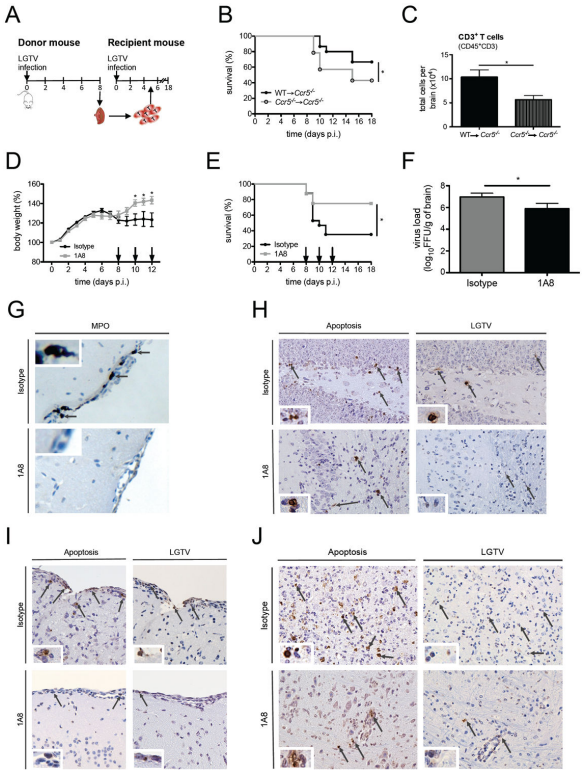

Figure 6. Early recruitment of T cells and the absence of neutrophils in the CNS of LGTV-infected Ccr5-deficient mice result in decreased neuropathology

(A) A schematic diagram of the experimental layout for the T cell adoptive transfer experiment is displayed. Donor mice (WT or *Ccr5*$^{-/-}$) were infected with LGTV, and T cells were isolated from spleens harvested on day 8 post infection. 1×10^{6} T cells were transferred into LGTV-infected recipient mice (*Ccr5*$^{-/-}$ mice) intravenously on day 5 post infection and evaluated for survival for 18 days **(B)**. Kaplan-Meier analysis of recipient mice with 18–20 *Ccr5*$^{-/-}$ mice per group. WT→*Ccr5*$^{-/-}$ mice received T cells from WT mice and *Ccr5*$^{-/-}$→*Ccr5*$^{-/-}$ received T cells from *Ccr5*$^{-/-}$ mice. **(C)** The total number of CD3^{+} T cells (CD45^{hi}CD3^{+}) was assessed by flow cytometry on day 8 post infection in the brains of *Ccr5*$^{-/-}$ mice receiving either WT or *Ccr5*$^{-/-}$ CD3^{+} T cells. Data are shown as mean ±SD for 4–6 mice per group. **(D)** Body weight was measured daily for isotype and anti-Ly6G (clone 1A8) treated LGTV-infected mice for 12 days post infection with 16-17 mice per group pooled from two independent experiments. **(E)** *Ccr5*$^{-/-}$ mice were injected with either isotype or 1A8 antibody, and survival was assessed by a Kaplan-Meier analysis through day 18 post infection with 16-17 mice per group pooled from two independent experiments. The arrows in C and D indicate the days when the antibody was administered. **(F)** The viral load was quantified in the brains of isotype or 1A8 antibody-treated mice on day 12 post infection. Shown is the mean ±SD from 7–8 mice per group on day 12 post infection from two independent experiments. **(G)** Immunohistochemical analysis was performed on paraffin-embedded brain sections for myeloperoxidase (MPO) from mice treated with isotype or 1A8 antibody on day 12 post infection. Immunohistochemical analysis was performed on paraffin-embedded brain sections after staining for apoptosis (TUNEL stain, left panels) or LGTV (right panels) in the **(H)** meninges, **(I)** hippocampus, and **(J)** deep

cortical layers for 3-5 mice per genotype and condition from two independent experiments. Representative images are shown at 20× magnification. * $p<0.05$.